Continental Shelf Research 117 (2016) 20–29

Contents lists available at ScienceDirect

Continental Shelf Research

journal homepage: www.elsevier.com/locate/csr

Research papers

Simulation of the effects of bottom topography on net primary production induced by riverine input

Yasuhiro Hoshiba*, Yasuhiro Yamanaka

Faculty of Environmental Earth Science, Hokkaido University N10W5, Kita-ku, Sapporo 060-0810, Japan

ARTICLE INFO

Article history:
Received 23 March 2015
Received in revised form
20 September 2015
Accepted 31 January 2016
Available online 1 February 2016

Keywords:
Biogeochemical cycles
3-D modeling
Riverine input
ROFI
Phytoplankton bloom
Bottom slope angle

ABSTRACT

Riverine input often leads to high biological productivity in coastal areas. In coastal areas termed as region of freshwater influence (ROFI), horizontal anticyclonic gyres and vertical circulation form by density differences between buoyant river water and sea water. Previous physical oceanography studies have shown that the horizontal pattern of anticyclonic gyres and the strength of vertical circulation are dependent on the bottom topography of ROFI. However, the dependencies of biogeochemical cycles such as the net primary production (NPP) on the bottom topography have not been verified. In order to clarify how the bottom topography affects the NPP in phytoplankton blooms caused by riverine input through the physical processes in ROFI, we used an ocean general circulation model (OGCM) including a simple ecosystem model and conducted several case studies varying the bottom slope angle in the ideal settings. We estimated NPP categorized into three nutrients supplied from the river, the sea-subsurface layer and via regeneration: RI-NPP, S-NPP and RE-NPP. S-NPP and RE-NPP are larger and smaller with a steeper slope, respectively, while RI-NPP is not affected by the slope angle. As a result, total NPP is weakly dependent on the slope angle, *i.e.*, because S- and RE-NPPs cancel each other out through two physical processes, (1) S-NPP is controlled by the strength of the vertical circulation and (2) RE-NPP is controlled by the shape of the horizontal gyre, which both vary with the bottom slope angle. We also conducted realistic simulations for Ishikari Bay, Japan and confirmed a similar dependency to that in the above ideal settings. That is, the simulation results are consistent with the regime of ideal settings and show that RI- and RE-NPPs are important variables for Ishikari Bay which has a gentle slope.

1. Introduction

Rivers transport both fresh water and nutrients from the land to the sea. Discharge from the river mouth influences adjacent coastal areas where biological productivity is high. Fresh water is supplied as a buoyant input into large areas of shelf seas adjacent to estuaries which were termed as region of freshwater influence (ROFI) by Simpson (1997). ROFIs play an important role in coastal regions through physical, biogeochemical and ecological functions (Lihan et al., 2008). Rivers directly supply dissolved inorganic nutrients to ocean system. Indirectly, buoyant freshwater inputs induce horizontal river plumes and vertical upwellings which transport nutrients from the deeper nutrient-rich layer to the surface layer. That is, net primary production (NPP) with nutrient cycles in ROFI is determined by these complex physical and biogeochemical processes above.

In ROFI, plankton blooms often occur especially when flooding occurs due to snowmelt and/or heavy rains (*e.g.*, Agboola et al., 2009). Hoshiba and Yamanaka (2013) investigated the temporal and spatial shift of phytoplankton blooms induced by large amounts of riverine discharge. The study found that NPP is induced by nutrient supplies not only from the river input but also from the subsurface layer through upwelling and by regeneration. We expect that the nutrient supplies are controlled by the topographic features of ROFIs such as the bottom slope angle of the continental shelf, because two important physical processes are dependent on the topography as follows.

Firstly, buoyant water inputs with low salinity induce vertical circulation, composed of surface water flows from the coast to the offshore and subsurface counter-flows with upwelling near the coast (Rattray and Hansen, 1962). The strength of the vertical circulation depends on the depth of ROFI, the density difference between the river water and the coastal sea water, and the coefficient of eddy viscosity (Unoki, 1993). As the strength is proportional to the cube of depth of the flat bottom (Unoki, 1993), the vertical circulation is expected to depend strongly on the bottom slope angle.

* Corresponding author.
E-mail address: h-dragon@ees.hokudai.ac.jp (Y. Hoshiba).

http://dx.doi.org/10.1016/j.csr.2016.01.020

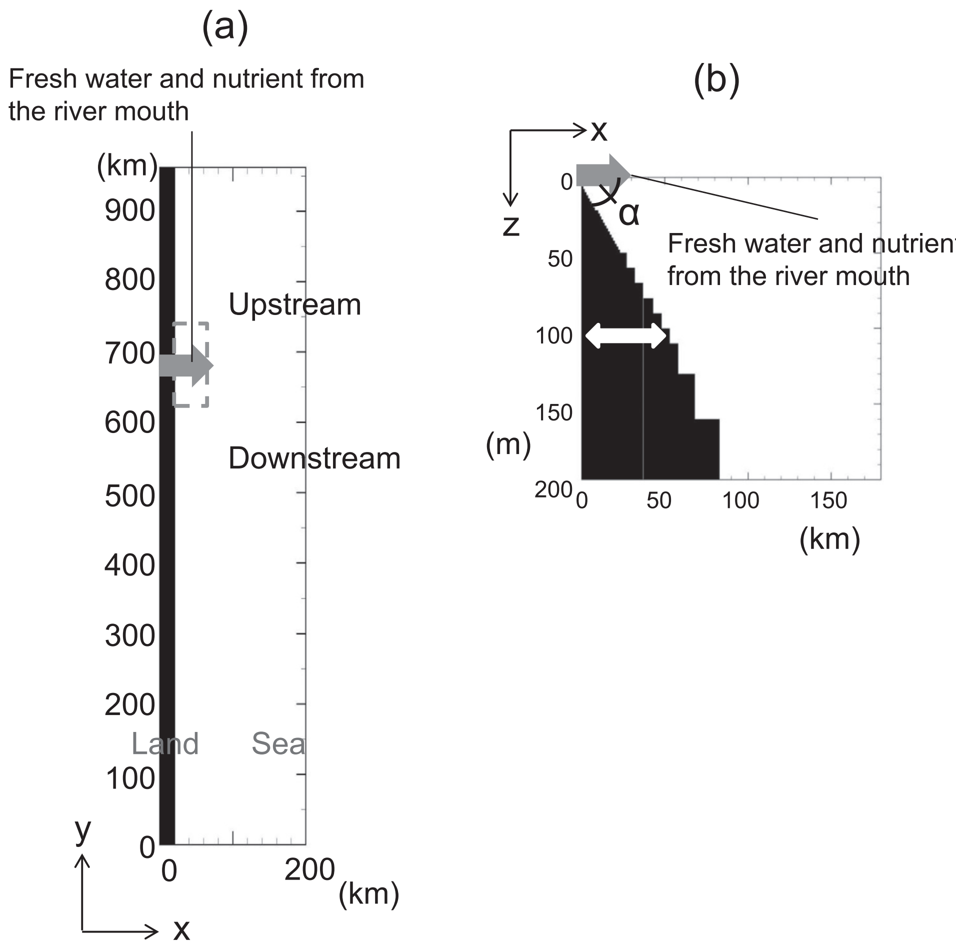

Fig. 1. (a) Horizontal geography and (b) vertical topography used in the model. The width of the river mouth is 3 km. The width of the region shallower than 100 m with the angle alpha was changed. The area surrounded by the dashed line shows the area drawn in Figs. 5 and 9.

Table 1
Experiments.

Experiment No.	1	2	3	4	5[a]	6	7	8	9	10
Shallow width (km)[b]	90	80	70	60	50	40	30	20	10	0
Slope angle α (deg)[c]	0.06	0.07	0.08	0.09	0.11	0.13	0.16	0.27	0.54	–

[a] Experiment No. 5 is the control case approximating the actual shallow area width.
[b] Width of the region shallower than 100 m depth (km) (see Fig. 1).
[c] Slope angle is determined from the shallow area width.

Table 2
Sinking rates of detritus in Exp. 1 and 8.

Sinking rate (m/day)	2	10	20	50	100	200

1): Experiments listed in Table 1 use 20 m/day.

Secondly, fresh water from rivers also induces horizontal river plumes with anticyclonic gyres due to geostrophic adjustment (*e.g.*, Isobe, 2005). There are previous studies related to the physics of the anticyclonic gyre enlarging with the bottom topography, for example, the horizontal gyre tends to be strongly trapped on the shelf and be suppressed toward the offshore direction in areas with a gently sloping bottom topography (Fig. S1; Tanaka et al., 2009).

In this study, we applied an OGCM with an ecosystem model to clarify how the bottom slope angle controls the NPP in phytoplankton blooms. Model case studies varying the bottom slope angle show how physical processes of vertical circulation and horizontal gyre control various nutrient supplies from the river,

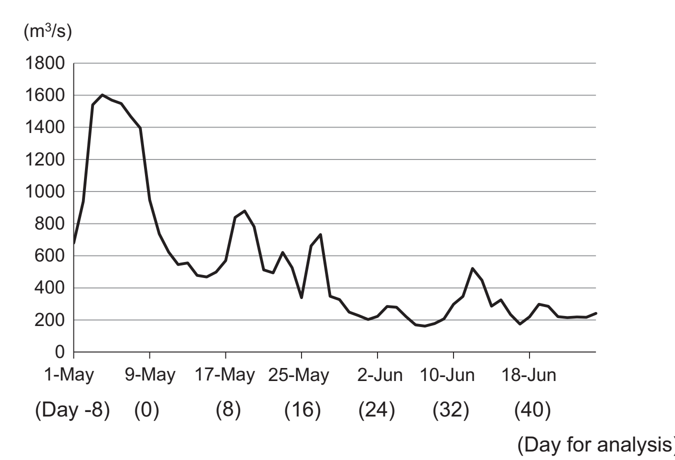

Fig. 2. River discharge observed at Ishikari Ohashi located 22.6 km from the river mouth of Ishikari River in Hokkaido, Japan in May to June, 2007 (Ministry of Land, Infrastructure, Transport and Tourism, Japan: http://www1.river.go.jp/). Days in parentheses show the day number in the simulation analysis in this study.

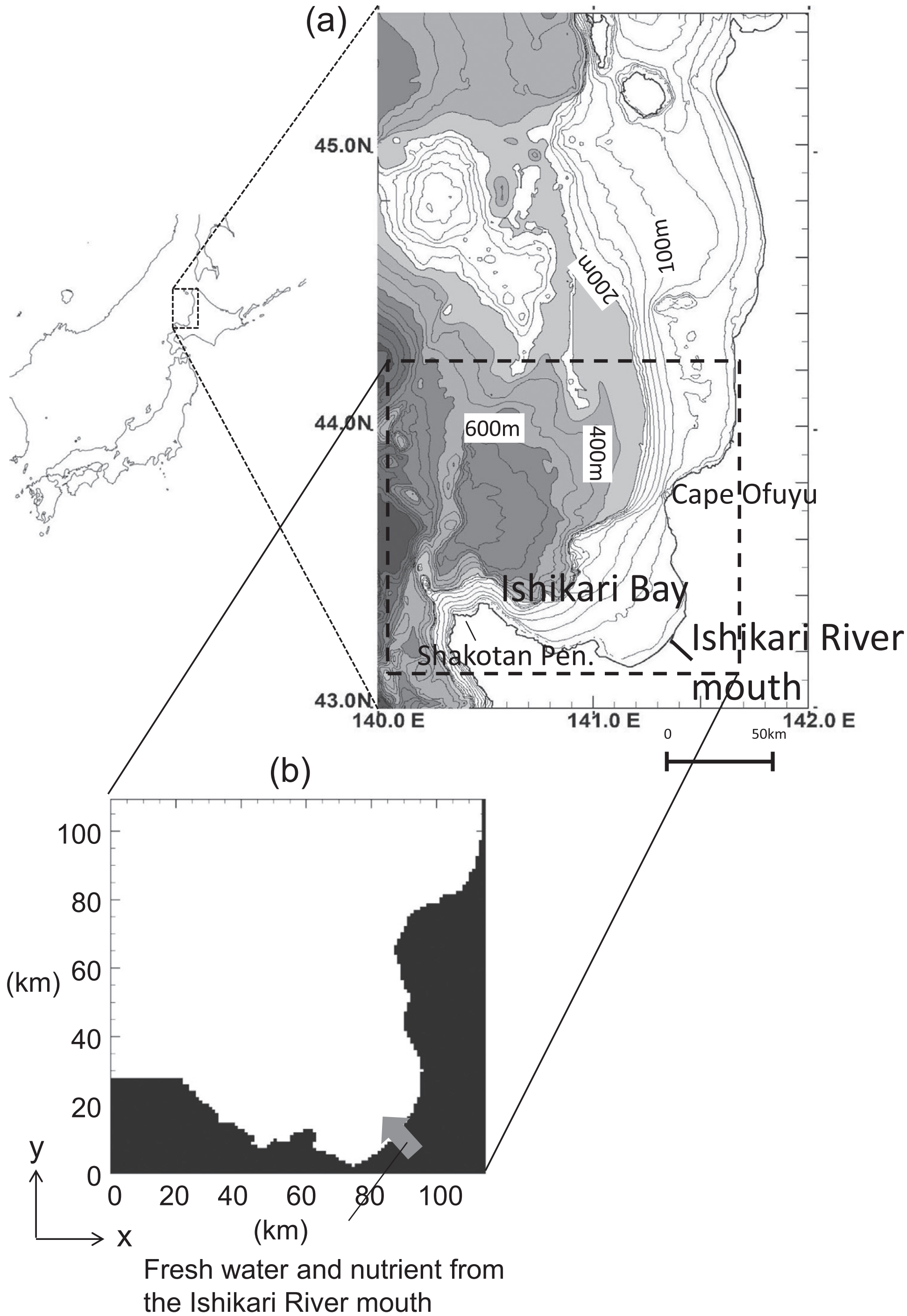

Fig. 3. (a) Geography and topography off the west coast of Hokkaido, Japan. (b) Horizontal geography of Ishikari Bay used in the model.

the sea-subsurface layer and regeneration. We used two sets of topographies: (1) idealized setting as the same in Hoshiba and Yamanaka (2013) except varying the bottom slope angle and (2) realistic topography, Ishikari Bay in Hokkaido, Japan with realistic topography and flat bottom. Ishikari Bay is one of the ROFIs in the subarctic region, and the Ishikari River discharges fresh water and nutrients into Ishikari Bay. Latter set is conducted to confirm the validity of the dependence of nutrient supplies on the bottom slope angle obtained by idealized setting in a realistic situation.

2. Model and simulations

2.1. Idealized setting

The model used in this study is the same as in Hoshiba and Yamanaka (2013). The simple ecosystem part based on the four-compartment version in Yoshikawa et al. (2005) was incorporated into an OGCM, COCO ver. 4.0 (Hasumi, 2002). The four prognostic variables in the ecosystem part are composed of nutrient,

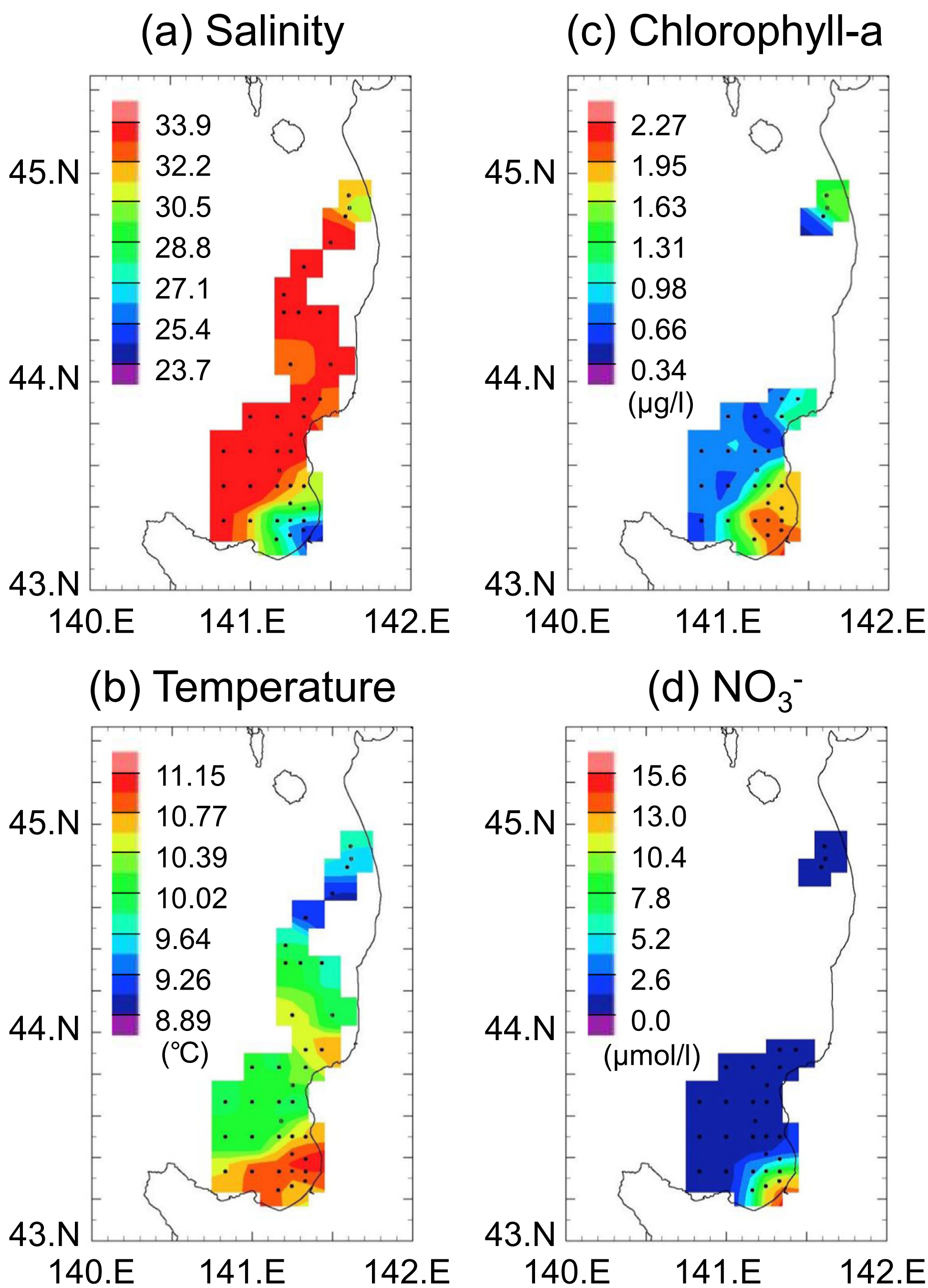

Fig. 4. The Gaussian interpolation of observation data in May, 2007 (provided by Y. Isoda and I. Kudo, *personal communication*), the horizontal distributions of (a) salinity, (b) temperature, (c) chlorophyll-a and (d) nitrate in the surface layer ((a) and (b) are at 2 m depth, and (c) and (d) are at 0 m), with dots that shows observation points.

phytoplankton, zooplankton and detritus (Fig. S2). We dealt with fresh water and nutrients flowing from a river into the ocean which has a simplified rectangular domain (Fig. 1(a) and (b)) on the f-plane (*i.e.*, assuming the Coriolis force at a fixed latitude, about 43 °N). The model domain is large enough not to affect the river plume. The horizontal grid sizes are approximately 1 km (*x*-direction) and increasing from 1 km near the river mouth to 20 km far from the river mouth (*y*-direction). The model has 34 vertical layers with the layer thickness increasing from 2 m at the surface to 40 m at the bottom. The depth to the ocean floor varied from 6 m in the nearshore area to 200 m for the offshore area (Fig. 1(b)). The horizontal diffusion coefficient and the diffusion coefficient along and across the isopycnals were set to typical values in the model 1.0×10^5 cm^2/s and 1.0×10^6 cm^2/s, respectively. The vertical diffusion coefficient was 0.5 cm^2/s that is a somewhat large coefficient relative to the typical value (about 0.1 cm^2/s; Tsujino et al., 2000) due to the effects of vertical mixing in coastal regions.

For idealized setting, we conducted ten experiments (Table 1) changing the bottom slope angle (α in Fig. 1(b)). We call Experiment 5 the control case, with a slope angle approximating the actual slope angle of Ishikari Bay. The sinking rate of detritus used is 20 m/day, except in Exp. 1 and 8 in which the sinking rate of detritus is changed (Table 2) referring to Syvitski et al. (1995) and Kriest (2002).

As for the freshwater input instead of that in Hoshiba and Yamanaka (2013), we used the river discharge of the Ishikari River, Japan, which is the observed data with a large discharge by heavy

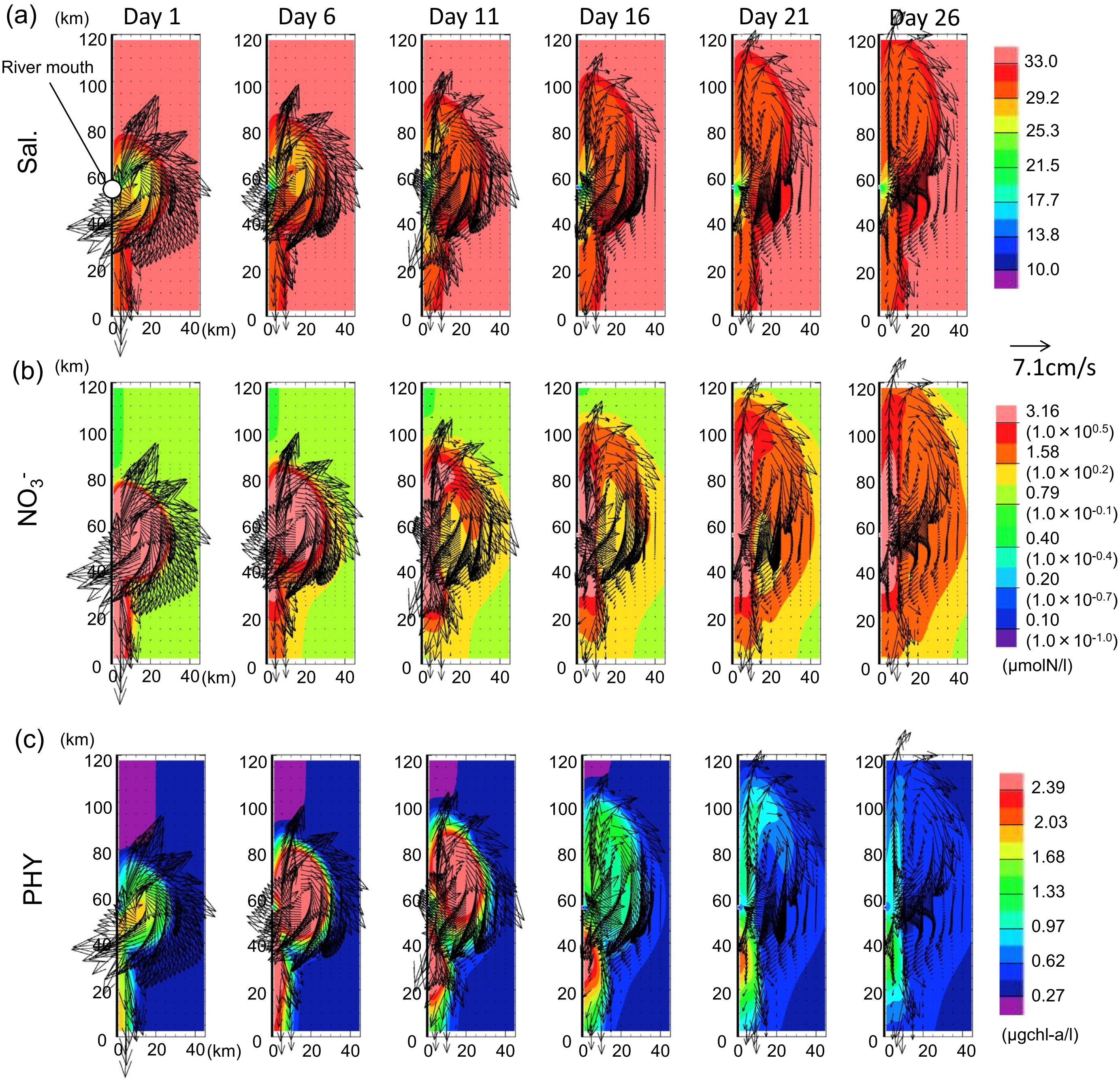

Fig. 5. The control case, the horizontal distributions of (a) salinity, (b) nitrate and (c) phytoplankton in the surface layer (1 m depth), with current velocity field vectors drawn at intervals of five grids. PHY is drawn as chlorophyll-a unit multiplied by the nitrogen–chlorophyll ratio of 1:1.325 (Yoshikawa et al., 2005).

rainfall of several days in addition to spring snowmelt in May, 2007 (Fig. 2). Nitrate concentration in the fresh water is 1.0 mg/l, a typical value representative of rivers in Hokkaido, Japan (Tachibana et al., 2001; Ileva et al., 2009). These are inputted into the river mouth region of 20 km × 3 km. We started the simulation on May 1st to June 28th, and analyzed from May 9th, a duration of 50 days.

The NPP in each experiment subtracted by that in the experiment without riverine input was regarded as the NPP driven by riverine input (hereafter we call NPP). To identify the nutrient sources utilized by NPP, we introduced nitrates categorized into three sources from the river, the sea-subsurface layer and via regeneration (hereafter, we term these as river- nitrate, RI-nitrate; subsurface- nitrate, S-nitrate; and regenerated nitrate, RE-nitrate, respectively). RI-nitrate is the river nutrient input integrated over time (*i.e.*, there is no RI-nitrate as the initial condition).

2.2. Realistic setting for Ishikari bay

Ishikari Bay is defined here as the area inside of a straight line linking Cape Ofuyu to the Shakotan Peninsula (Fig. 3(a)), in which the bottom is less than 100 m depth as a gentle coastal shelf. In the area offshore of Ishikari Bay, the Tsushima Warm Current flows along the steep continental slope from southwest to northeast. There is a small nutrient supply from the Tsushima Warm Current with nutrient-poor water to the Ishikari Bay (Yoshida et al., 1977). Probably, NPP is controlled by nutrient supplies from the Ishikari River rather than from the Tsushima Warm Current. Ishikari River has the largest discharge in Hokkaido, with a river mouth of about 1.5 km width and 2.8 m mean depth.

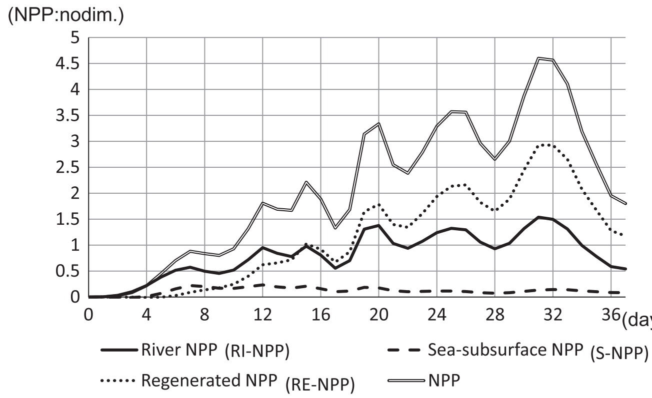

Fig. 6. Time series of the normalized Net Primary Productions, NPPs, driven by river input in the calculation domain, that is, NPPs in the control case subtracted by that in the no flux case. NPPs are categorized into three sources: river (solid line), sea- subsurface (dashed line), and regenerated (dotted line) and normalized by the nitrate input, *i.e.*, nitrate of the daily mean in the control case.

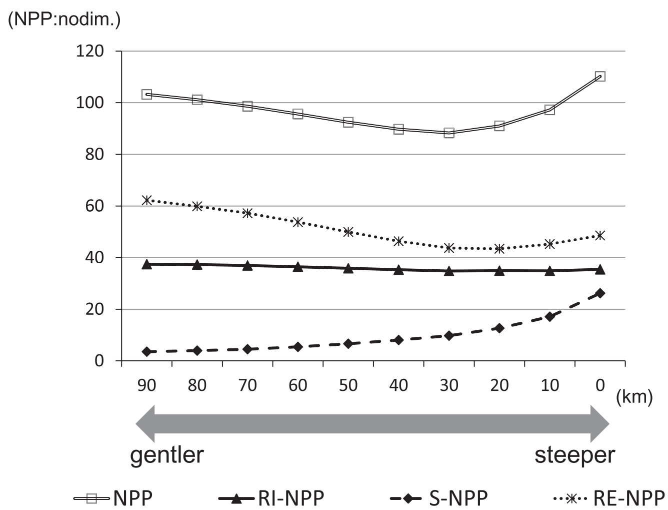

Fig. 7. Accumulated NPPs for 46 days in the cases changing in the bottom slope angle. The respective NPPs are subtracted and normalized as in Fig. 6. The *x*-axis shows the width of the region shallower than 100 m.

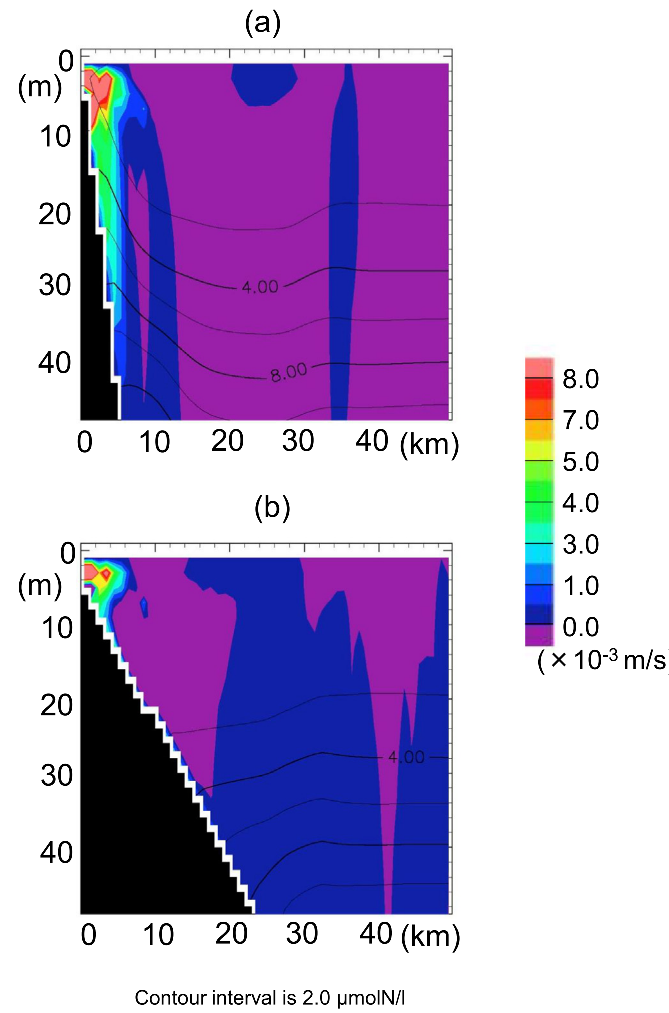

Fig. 8. (a) Vertical flow and sea-subsurface nitrate along the section at the river mouth in the steep slope case (Exp. 9; Day 13). (b) The same as in (a) except for the control case.

In the simulations, we took a large area outside Ishikari Bay, a square of sides of 110 km (Fig. 3(b)); the north and west boundaries were at 1900 km north and 450 km west from Ishikari Bay, which was large enough to cover the area of the flow of Tsushima Warm Current. The horizontal grid sizes are approximately 1 km in Ishikari Bay. The model has 43 vertical layers with thickness increasing from 2 m at the surface to 50 m at the bottom. The physical setting and values are the same as in Section 2.1 except the vertical viscosity and diffusivity that were determined using the turbulence closure level 2.5 scheme (Mellor and Yamada, 1982).

We conducted two experiments with (1) the realistic bottom topography, which is close to that of the control case (Table 1), and (2) the flat bottom of 100 m depth instead of realistic bottom topography shallower than 100 m depth to confirm the effect of the bottom slope angle.

We used the Gaussian-interpolated data of temperature, salinity and concentrations of nitrate and phytoplankton observed in 9th to 15th May, 2007 (as for physical data, Y. Isoda, *personal communication*; as for biogeochemical data, I. Kudo, *personal communication*) (Fig. 4). We conducted a 2-day spin-up of currents consistent with the temperature and salinity data above for geostrophic adjustment, combined with ecosystem components after a 3-month spin-up with the 4-days restoring to the above nitrate and phytoplankton concentrations with the currents after the above 2-day spin-up. We used the 4-days restoring to the above temperature and salinity data out of Ishikari Bay in the above spin-up and two experiments driven by the riverine discharge, to keep the flow of Tsushima Warm Current. We used the same riverine discharge and nitrate concentration in the idealized setting in Section 2.1, except the region of riverine-input of 2 km × 2 km for 50 days.

We did not deal with the effects of the tide, because the sum of the four major tidal components (M2+S2+K1+O1) is estimated to be only 17 cm at most in Ishikari Bay (Unoki, 1993).

3. Results

The low salinity (low density) water from the river mouth forms an anticyclonic gyre due to geostrophic adjustment in the control case (Fig. 5(a)). We team the left (right) side, by looking offshore from the river mouth, 'upstream' ('downstream'), according to previous studies (*e.g.*, McCreary et al., 1997; Yankovsky, 2000). The downstream is the direction of propagation of the Kelvin wave. Anticyclonic gyres often spread and propagate towards the upstream region (*e.g.*, major Siberian rivers in the Arctic; Weingartner et al., 1999, La Plata River; Matano and Palma, 2010, some rivers in Suo-Nada in Japan; Magome and Isobe, 2003).

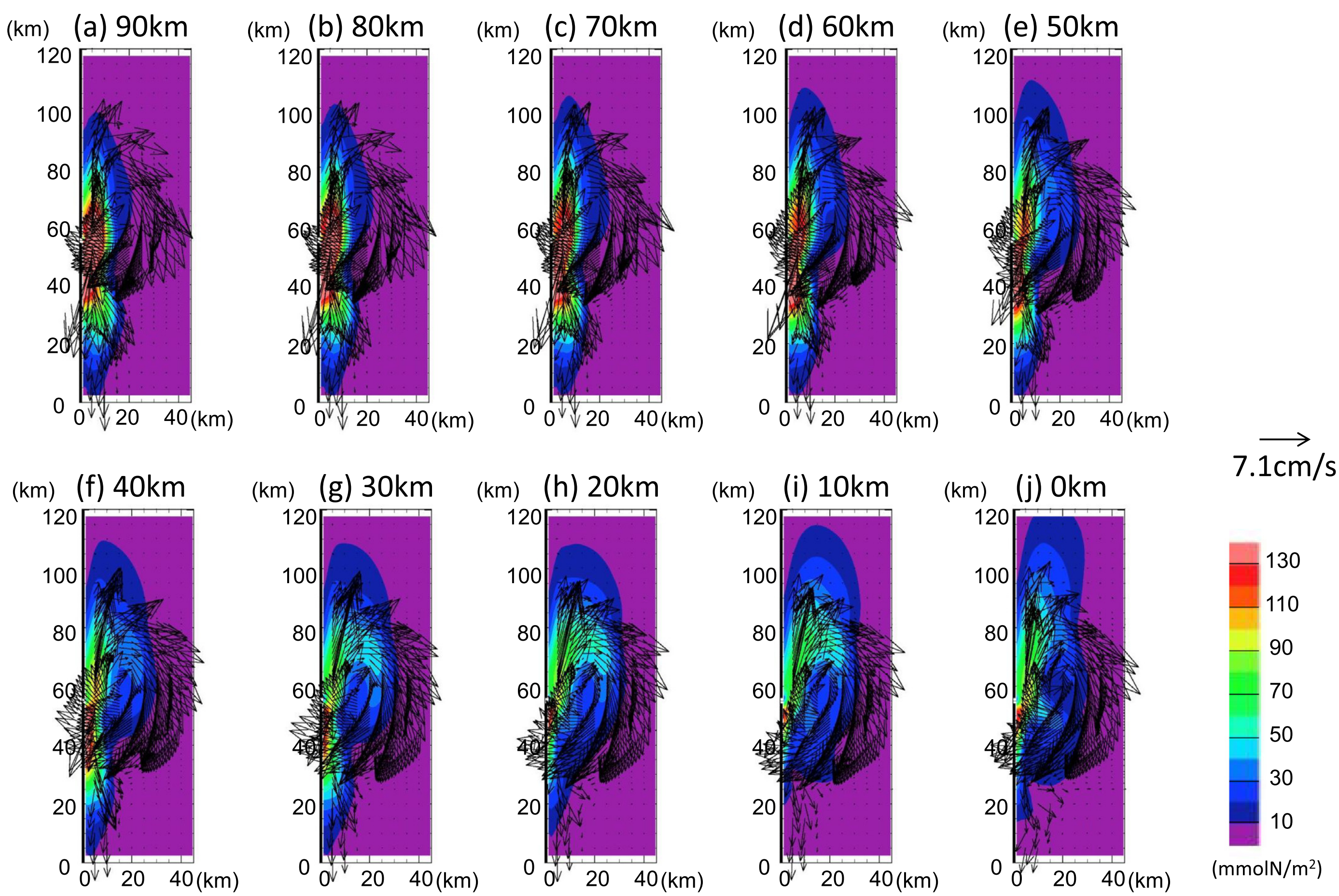

Fig. 9. Accumulated RI-NPPs vertically and temporally for 46 days. Vectors show current velocity field in the surface, drawn at intervals of five grids. The width of region shallower than 100 m changes from (a) 90 km to (j) 0 km.

Generally, the propagation to the upstream tends to occur, when the river mouth width is smaller than the internal deformation radius determined by the difference in density between the river water and sea water. Especially, the propagation occurs more when the internal deformation radius becomes larger due to flooding caused by snowmelt or heavy rainfall.

The anticyclonic (clockwise in the northern hemisphere) flows entrain the inflow from the river to the upstream direction. The buoyant water from the river is transported in order of upstream, offshore, and then downstream by the clockwise flows. The transported water is trapped against the coast and flows to the downstream region (Fig. 5(a); Day 1) as a Kelvin Wave (*e.g.*, Bowden, 1983). The anticyclonic gyre propagates to the upstream region as time progresses (Fig. 5(a); Day 6–26). After Day 11, the anticyclonic gyre enlarges to a certain extent in the upstream region and return flow toward the coast driven by the gyre is generated near the river mouth. The flow separates fresh water flowing from the river into the upstream and downstream sides. These flows are one of the factors to determine the horizontal distributions of the nitrate from the various sources. The horizontal distribution of high nitrate (Fig. 5(b)) is similar with that of fresh water until Day 6. However, the pattern for nitrate becomes gradually different from that of fresh water as time progresses. This is because nitrate has various sources: sea-subsurface and regenerated as well as from rivers. We introduced the nitrates colored by three sources from river (RI-nitrate), sea-subsurface water (S-nitrate) and regeneration (RE-nitrate), as mentioned in Section 2.

Phytoplankton utilize these nitrates, and blooms occur (Fig. 5 (c)). We estimated NPP categorized into the above three sources: river- NPP (RI-NPP), subsurface- NPP (S-NPP) and regenerated NPP (RE-NPP) in proportion to the nitrate uptake of the three sources. The rates of respective RI-, S- and RE-NPPs change with the experiment time in the control case (Fig. 6). RE- and S-nitrates as well as RI-nitrate are important for phytoplankton blooms. At the first stage, phytoplankton utilize in order of RI-, S- and RE-nitrates until Day 8. Secondly, the order is RI-, RE- and S-NPPs due to RE-NPP overtaking S-NPP from Day 9 to 14, and RE-NPP is the main factor of total NPP in the last stage (after Day 15). When total NPP counts as 100% by Day 46, the accumulated RI-, S- and RE-NPP is 39%, 7% and 54%, respectively. That is, NPP of the phytoplankton bloom is conducted through different nutrient sources.

4. Discussion

4.1. *Effects of the angle of bottom slope*

To clarify the impact of the bottom slope on phytoplankton blooms, we conducted case studies changing the bottom slope angle. Total NPP gradually decreases with the bottom slope becoming steeper until the 30 km case (Fig. 7; doublet), and NPP in the cases steeper than 30 km case are larger with a steeper slope. This is because different nutrient sources support NPP, the sum of RI-, S- and RE-NPPs. S-NPP is larger with a steeper slope (Fig. 7; black broken line). RE-NPP except 10 km and 0 km cases is smaller with a steeper slope (Fig. 7; dotted line). RI-NPP is almost independent of the slope angle (Fig. 7; solid line).

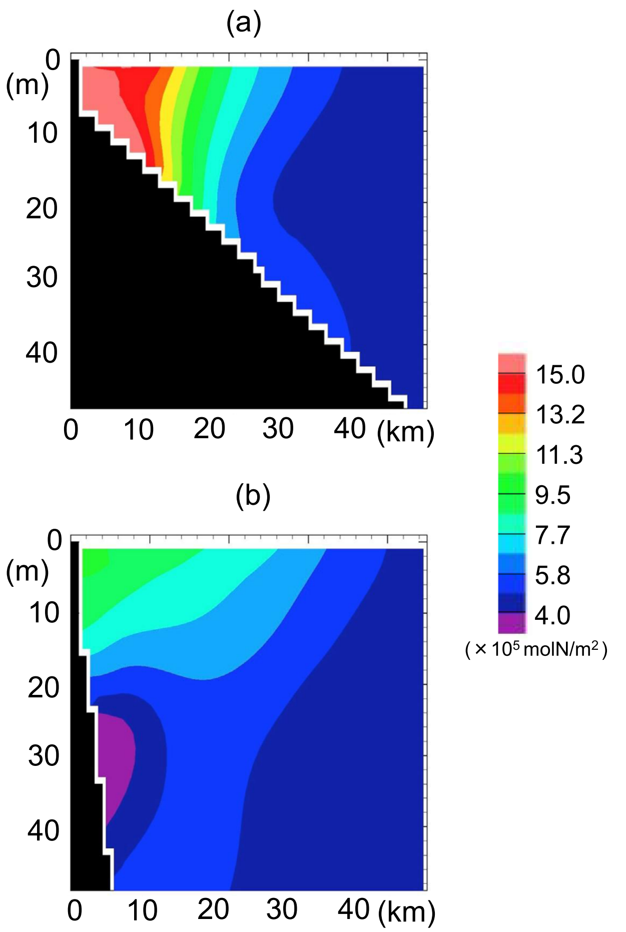

Fig. 10. (a) Amount of zonal RE-nitrate for 46 days in the gentle slope case (Exp. 1), subtracted by that in the no flux case. (b) The same as (a) except that in the steep slope case (Exp. 9).

Table 3
Tendencies of NPPs and physical conditions.

Slope angle	RI-NPP	S-NPP	RE-NPP	Upwelling	Width of horizontal gyre toward the offshore
steep	Unchanged	+	−	strong	broad
gentle	Unchanged	−	+	weak	narrow

The strength of vertical circulation is proportional to the cube of the depth, as mentioned in the introduction. Upwelling near the coast and its S-nitrate supply are stronger and larger with a steeper slope (Fig. 8). A previous study also shows that coastal upwelling in the South China Sea causes strong spatiotemporal variations among nutrient, phytoplankton and zooplankton (Gan et al., 2010).

While RI-NPP is not dependent on the slope angle, its horizontal distribution changes with the slope angles due to the change in the horizontal gyre (Fig. 9). In the gentle slope cases, the horizontal gyre tends to be strongly trapped along the coast (Tanaka et al., 2009), and the high RI-NPP area is also concentrated near the coast.

It is generally expected that RE-NPP increases with the higher RI- and S-NPPs, because higher NPP leads to high concentration of RE-nitrate through production and decomposition of organic matter. However, RE-NPPs are large despite the small S-NPPs in the gentle slope cases, compared with those in the steep slope cases. This is because phytoplankton in the gentler slope easily use RE-nitrates concentrated near the coast due to the shallower depth and the horizontal gyre trapped along the coast (Fig. 10).

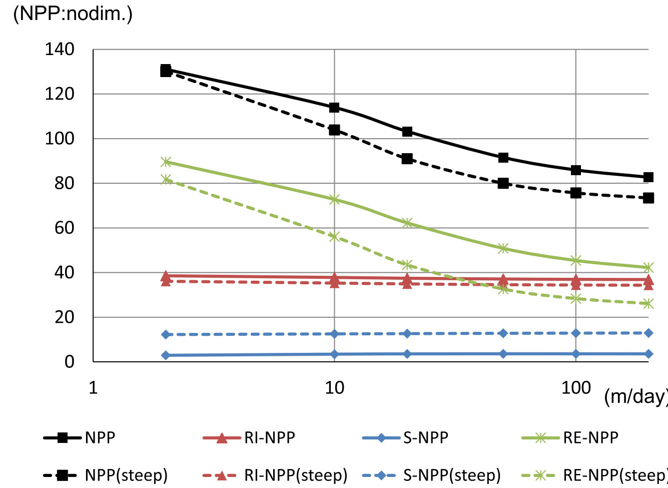

Fig. 11. Accumulated NPPs for 46 days in the gentle slope (solid lines) and the steep slope (dashed lines) cases. The *x*-axis shows the sinking rate of detritus (m/day). (For interpretation of the references to color in this figure, the reader is referred to the web version of this article.)

Therefore, S-NPP in the steep slope cases is larger due to strong upwelling induced by vertical circulation, while RE-NPP in the gentle slope is large due to the shallower depth and horizontal gyre trapped. As a result, total NPP (= sum of RI-, S- and RE-NPPs) are weakly dependent on the slope angle, though the ratios of its components are dependent (Fig. 7 and Table 3).

4.2. Effects of change of the detritus-sinking rate

To confirm the findings about dependencies of RI-, S- and RE-NPPs above on the slope angle, we conducted an additional five experiments changing the sinking rate of detritus from 2 m/day to 200 m/day (instead of original 20 m/day), for Exp. 1 as a gentle slope case and Exp. 8 as a steep slope case, respectively.

Change in the sinking rate has much influence on RE-NPP (Fig. 11). Since a higher sinking rate of detritus leads to the conversion of detritus into RE-nitrate at deeper depths, RE-nitrate supply from the subsurface decreases and then RE-NPP decreases.

RE-nitrate is easily used in the gentler slope due to the conversion in the shallower depth, as mentioned above. That is even if there is a high sinking rate, the conversion occurs on the shallow ocean floor. As a result, the dependency of the sinking rate on RE-NPPs in the gentle case (Green solid line in Fig. 11) is weaker than those in the steep case (Green broken line in Fig. 11).

Since RI-, S- and RE-NPPs in the gentle case are kept smaller or larger than those in the steep case (*i.e.*, all solid and broken lines are not crossed for each other), the findings in the subsection such as their dependencies on the slope angle hold, even for different sinking rates from the original one.

4.3. Realistic model simulations (Ishikari bay)

We also conducted realistic simulations for Ishikari Bay. Tsushima Warm Current forced by geostrophic balance flows from the southwest to the northeast, offshore of Ishikari Bay (Fig. 12). The main current axis does not penetrate into the inside of Ishikari Bay. Anticyclonic gyre occurs in Ishikari Bay, and low salinity water (green-colored area in Fig. 12) from the Ishikari River is transported in order of the upstream and offshore region with time, although the low salinity region toward the offshore direction shrinks after Day 13, due to the reduced discharge of the Ishikari River (Fig. 2). Low salinity region (orange to red region in Fig. 12;

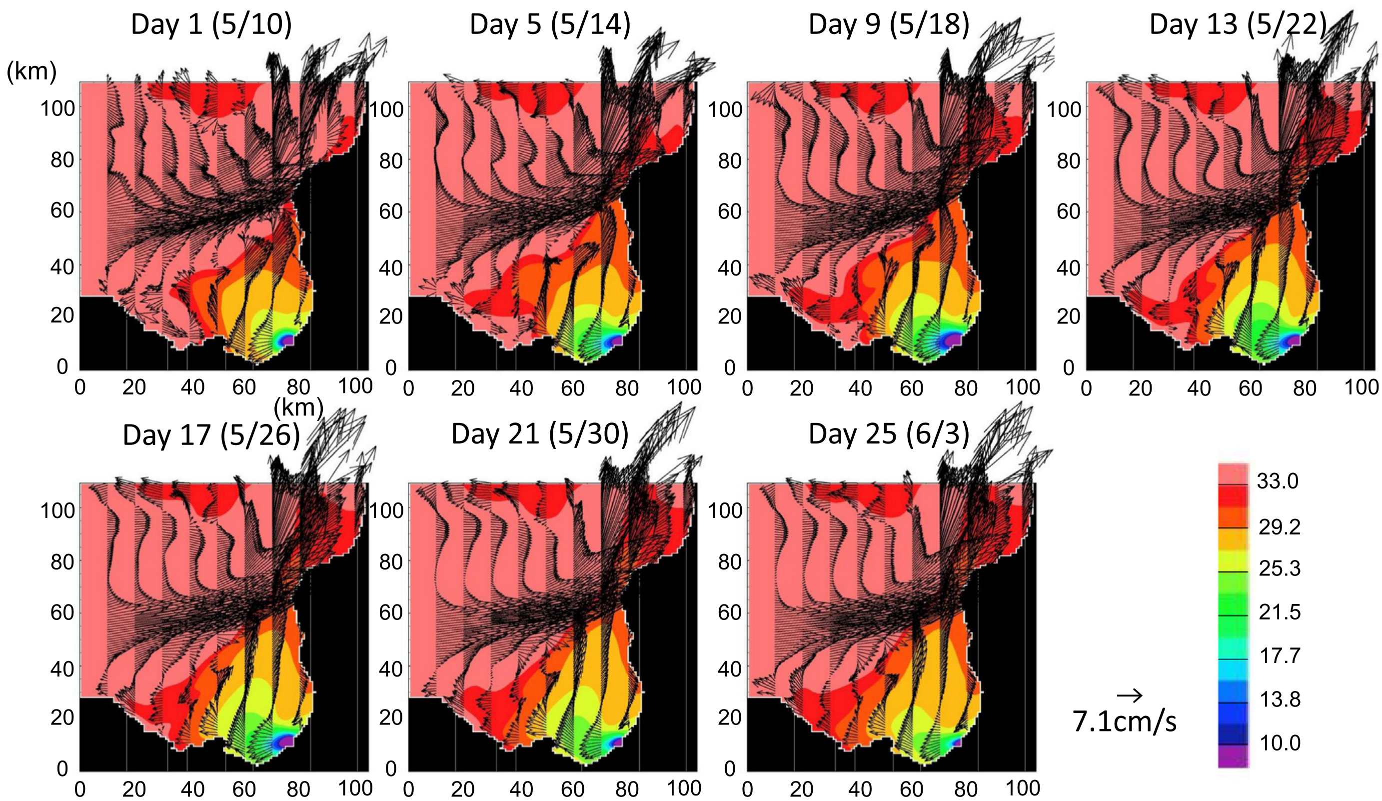

Fig. 12. In the Ishikari Bay case, the horizontal distributions of salinity in the surface layer (1 m depth), with current velocity field whose vectors are drawn at intervals of ten grids (For interpretation of the references to color in this figure, the reader is referred to the web version of this article.).

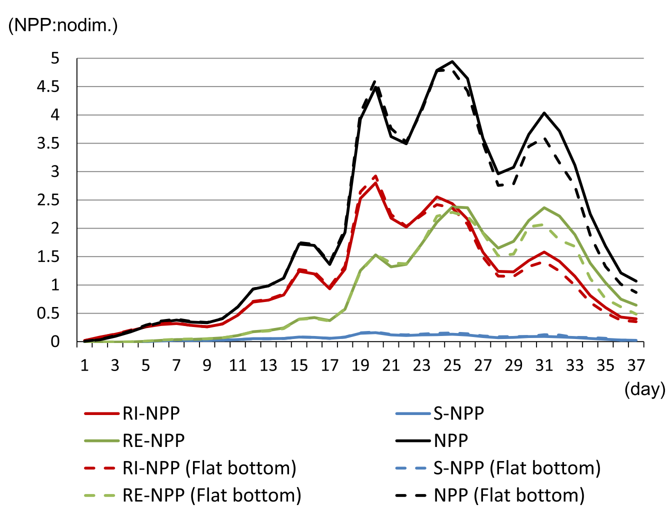

Fig. 13. The same as Fig. 6 except those in Ishikari Bay and those in flat bottom cases. Solid (dashed) lines show the Ishikari Bay (flat bottom) case.

29.2∼33.0) keeps to propagate to the upstream from the river mouth, which is the similar transition pattern to that in the control case (Fig. 5(a)).

We estimated how much of the nitrates are consumed in Ishikari Bay case (solid lines in Fig. 13). Not only riverine nutrient input of the Ishikari River but also regeneration on the shelf causes phytoplankton blooms in Ishikari Bay due to flooding of the Ishikari River. That is, the time shift of the main nutrient source from RI- to RE-NPPs is similar to that in the control case (Fig. 6). S-NPP in Ishikari Bay case is much smaller than that in the control case, due to the nutrient poor environment outside of Ishikari Bay where the Tsushima Warm Current transports low nutrient-water from the south. The accumulated RI-, S- and RE-NPPs until Day 46 are 54%, 3% and 43%, respectively. These percentages are consistent with findings in previous studies (Agboola et al., 2010; Agboola and Kudo, 2014). Agboola et al. (2010) implied that Ishikari Bay is considerably influenced by a lot of nutrient input from the Ishikari River (*i.e.*, consistent with the large percentage of RI-NPP). Agboola and Kudo (2014) concluded that the nutrient supply by estuarine circulation in Ishikari Bay is relatively smaller than that in other ROFIs (*i.e.*, consistent with the small percentage of S-NPP).

We compared RI-, S- and RE-NPPs in the cases with flat and realistic bottom topographies (Fig. 13). The relationships among RI-, S- and RE-NPPs with the flat and realistic bottoms are consistent relationships between the steep and gentle cases. That is, RE-NPP with the flat bottom has smaller values than with the realistic bottom, though S-NPP is very small with both bottom topographies due to the nutrient poor condition in the eutrophic waters outside of Ishikari Bay.

5. Summary and remarks

We used the ocean general circulation model (OGCM) including a simple ecosystem model developed in Hoshiba and Yamanaka (2013), to clarify the effect of the bottom topography on the NPP in phytoplankton blooms caused by riverine input in region of freshwater influence (ROFI).

We estimated NPP categorized into three sources from the river, the sea-subsurface layer and via regeneration: RI-NPP, S-NPP and RE-NPP. S-NPP in the steep slope cases is larger due to strong upwelling induced by vertical circulation, while RE-NPP in the gentle slope is large due to the shallower depth and horizontal gyre trapped. As a result, total NPP (=sum of RI-, S- and RE-NPPs) is weakly dependent on the slope angle, though the ratios of its components are dependent on the slope angle. We also confirmed that these dependencies on the slope angle hold, even over an extensive range of sinking rates.

We also conducted realistic simulations for Ishikari Bay. The relationships among RI-, S- and RE-NPPs with the flat and realistic bottoms in the Ishikari Bay are consistent with the relationships between the steep and the gentle cases, although S-NPP is very small due to the nutrient poor waters outside of Ishikari Bay.

We showed the response of NPP induced by riverine input in Ishikari Bay, as just an example. For future studies, we should investigate other factors such as the amount and duration of riverine input, and other types of ROFIs and apply to many realistic topographies, to understand how to determine NPPs in the various ROFI.

Acknowledgments

We deeply thank to Dr. Isao Kudo of the Faculty of Environmental Earth Science, Hokkaido University and Dr. Yutaka Isoda of the Faculty of Fisheries Sciences, Hokkaido University for providing a lot of observation data on Ishikari Bay. River discharge of the Ishikari River in 2007 was obtained from Water Information System by Ministry of Land, Infrastructure, Transport and Tourism, Japan. Yasuhiro Hoshiba was supported by the research project "the Development of mitigation and adaptation techniques to global warming" in Ministry of Agriculture, Forestry and Fisheries of Japan. Yasuhiro Hoshiba and Yasuhiro Yamanaka were also supported by Core Research for Evolutional Science and Technology (CREST), Japan Science and Technology Agency (JST).

Appendix A. Supplementary material

Supplementary data associated with this article can be found in the online version at http://dx.doi.org/10.1016/j.csr.2016.01.020.

References

Agboola, J.I., Yoshi, S., Kudo, I., 2009. Seasonal change of riverine nutrients and distribution of chlorophyll a in Ishikari Bay, subarctic oligotrophic coastal environment of Japan. La Mer 47, 1–17.
Agboola, J.I., Uchimiya, M., Kudo, I., Kido, K., Osawa, M., 2010. Dynamics of pelagic variables in two contrasting coastal systems in the western Hokkaido coast off Otaru port, Japan. Estuar. Coast. Shelf Sci. 86, 477–484.
Agboola, J.I., Kudo, I., 2014. Different contributions of riverine and oceanic nutrient fluxes supporting primary production in Ishikari Bay. Cont. Shelf Res. 88, 140–150.
Bowden, K.F., 1983. Physical Oceanography of Coastal Waters. John Wiley, United States, p. 302.
Gan, J., Lu, Z., Dai, M., Cheung, A.Y.Y., Liu, H., Harrison, P., 2010. Biological response to intensified upwelling and to a river plume in the northeastern South China Sea: a modeling study. J. Geophys. Res. 115, C09001.
Hasumi, H., 2002. Sensitivity of the global thermohaline circulation to interbasin freshwater transport by the atmosphere and the Bering Strait throughflow. J. Clim. 15, 2516–2526.
Hoshiba, Y., Yamanaka, Y., 2013. Along-coast shifts of plankton blooms driven by riverine inputs of nutrients and fresh water onto the coastal shelf: a model simulation. J. Oceanogr. 69, 753–767.
Ileva, N.Y., Shibata, H., Satoh, F., Sasa, K., Ueda, H., 2009. Relationship between the riverine nitrate-nitrogen concentration and the land use in the Teshio River watershed, north Japan. Sustain. Sci. 4, 189–198.
Isobe, A., 2005. Ballooning of river-plume bulge and its stabilization by tidal currents. J. Phys. Oceanogr. 35, 2337–2351.
Kriest, I., 2002. Different parameterizations of marine snow in a 1D-model and their influence on representation of marine snow, nitrogen budget and sedimentation. Deep-Sea Res. Part I 49, 2133–2162.
Lihan, T., Saitoh, S., Iida, T., Hirawake, T., Iida, K., 2008. Satellite-measured temporal and spatial variability of the Tokachi River plume. Estuar. Coast. Shelf Sci. 78, 237–249.
Magome, S., Isobe, A., 2003. Current structure and behavior of the river plume in Suo-Nada. J. Oceanogr. 59, 833–843.
Matano, P.R., Palma, E.D., 2010. The upstream spreading of bottom-trapped plumes. J. Phys. Oceanogr. 40, 1631–1650.
McCreary, J.P., Zhang, S., Shetye, S.R., 1997. Coastal circulations driven by river outflow in variable-density 1½-layer model. J. Geophys. Res. 102, 15535–15554.
Mellor, G.L., Yamada, T., 1982. Development of a turbulence closure model for geophysical fluid problems. Rev. Geophys. Space Phys. 20, 851–875.
Rattray, M., Hansen, D.V., 1962. A similarity solution for circulation in an estuary. J. Mar. Res. 20, 121–133.
Simpson, J.H., 1997. Physical processes in the ROFI regime. J. Mar. Syst. 12, 3–15.
Syvitski, J.P.M., Asprey, K.W., Leblanc, K.W.G., 1995. In-situ characteristics of particles settling within a deep-water estuary. Deep-Sea Res. Part II 42, 223–256.
Tachibana, H., Yamamoto, K., Yoshizawa, K., Magara, Y., 2001. Non-point pollution of Ishikari River, Hokkaido, Japan. Water Sci. Technol. 44, 1–8.
Tanaka, K., Michida, Y., Komatsu, T., Ishigami, K., 2009. Spreading of river water in Suruga Bay. J. Oceanogr. 65, 165–177.
Tsujino, H., Hasumi, H., Suginohara, N., 2000. Deep Pacific circulation controlled by vertical diffusivity at the lower thermocline depths. J. Phys. Oceanogr. 30, 2853–2865.
Unoki, S., 1993. Engan no Kaiyo Butsurigaku (Physical oceanography in coastal regions). Tokai University Press, Japan, p. 672.
Weingartner, T.J., Danielson, S., Sasaki, Y., Pavlov, V., Kulakov, M., 1999. The Siberian Coastal Current: a wind and buoyant-forced Arctic coastal current. J. Geophys. Res. 104, 29697–29713.
Yankovsky, A.E., 2000. The cyclonic turning and propagation of buoyant coastal discharge along the shelf. J. Mar. Res. 58, 585–607.
Yoshida, K., Domon, K., Watanabe, T., 1977. Physical and chemical conditions on the inshore fishing grounds in Ishikari Bay (in Japanese with English abstract). Sci. Rep. Hokkaido Fish. Exp. Stn. 34, 1–6.
Yoshikawa, C., Yamanaka, Y., Nakatsuka, T., 2005. An ecosystem model including nitrogen isotopes: perspectives on a study of the marine nitrogen cycle. J. Oceanogr. 61, 921–942.